

B

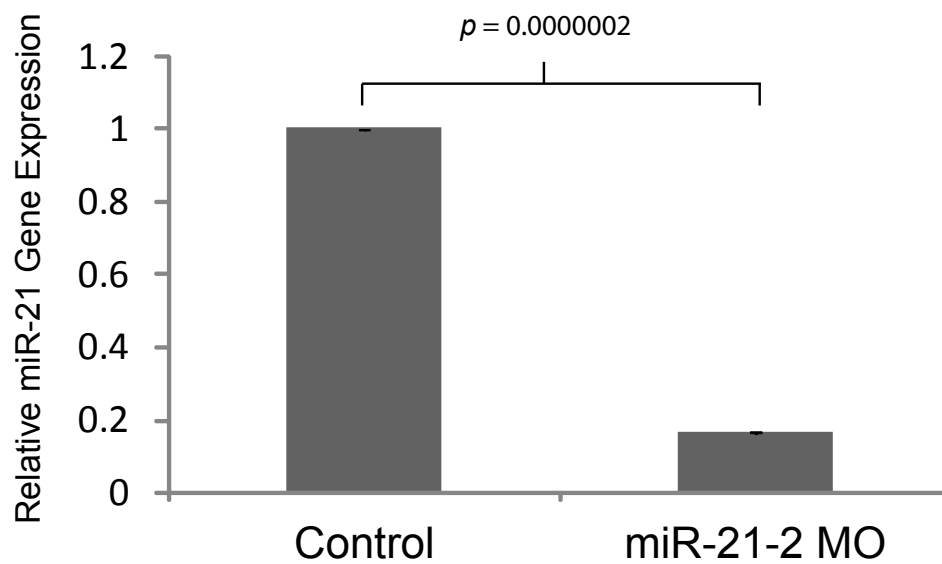


Fig. S1. miR-21 knockdown results in accumulation of miR-21 precursor and loss of mature miR-21. (A) Northern blot for short RNA molecules from control, miR-21-1 MO-injected, and miR-21-2 MO-injected embryos. Injection of miR-21-2 MO results in accumulation of the pre-miR-21 precursor (top band), which may be detected faintly in the miR-21-1 lane as well, but is absent from the control lane. (B) Injection of miR-21-2 MO causes a 90% reduction in the amount of mature miR-21 detectable by qPCR.

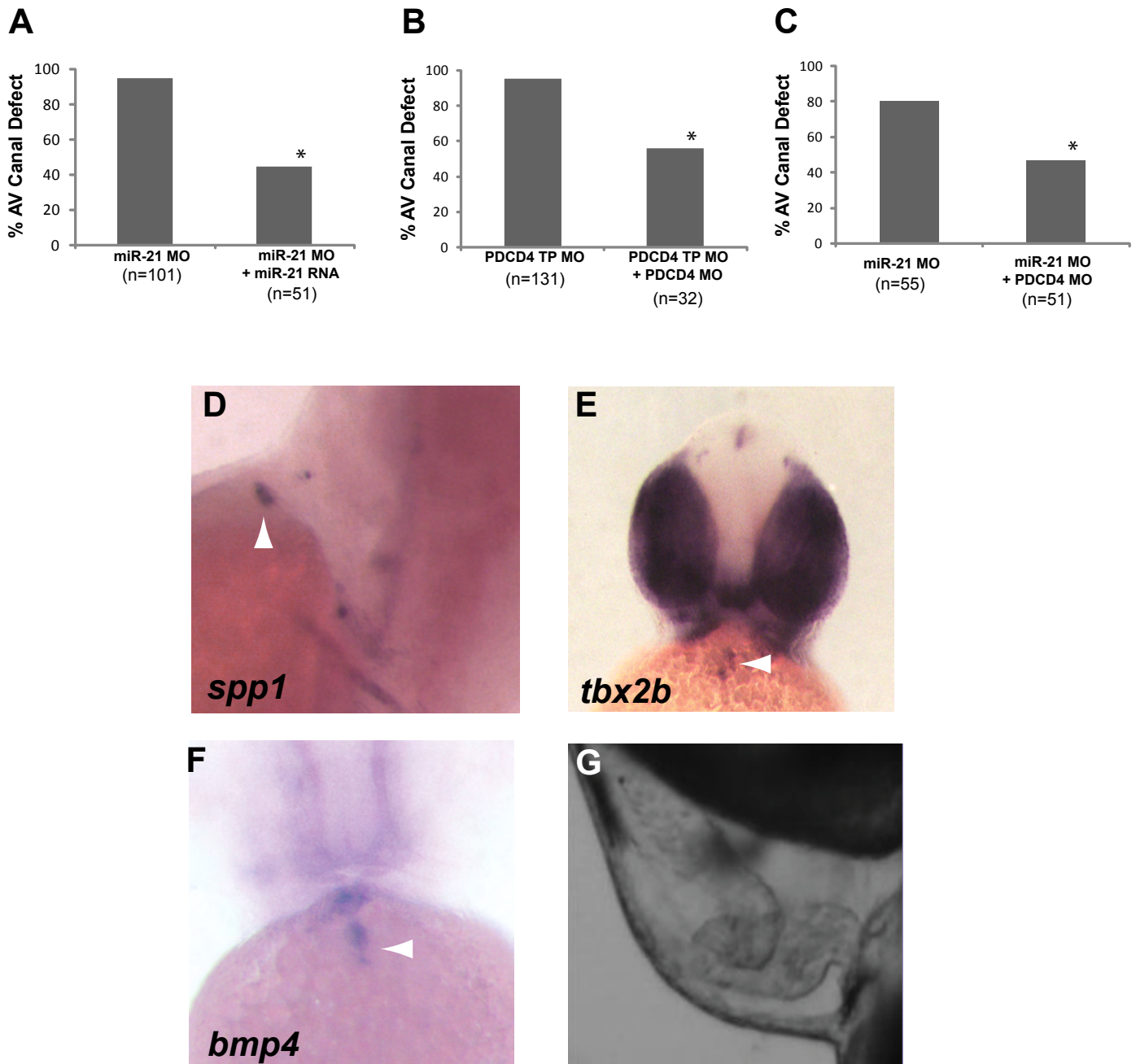


Fig. S2. Rescue of miR-21 phenotypes. (A) The miR-21 MO AVC defect is rescued by co-injecting mature miR-21 RNA into embryos. $*P=6 \times 10^{-12}$. (B) The PDCD4 target protector (TP) MO AVC defect is rescued by co-injecting a splice-acceptor PDCD4 MO. $*P=5 \times 10^{-8}$. (C) The miR-21 MO AVC defect is rescued by co-injecting a splice-acceptor PDCD4 MO into embryos. $*P=0.0005$. (D-F) Representative embryos demonstrating recovery of *in situ* expression patterns of the indicated genes after the rescue experiments performed above. The AVC is indicated by white arrowheads. (G) Representative embryonic heart demonstrating recovery of AV constriction and looping after the rescue experiments performed above.

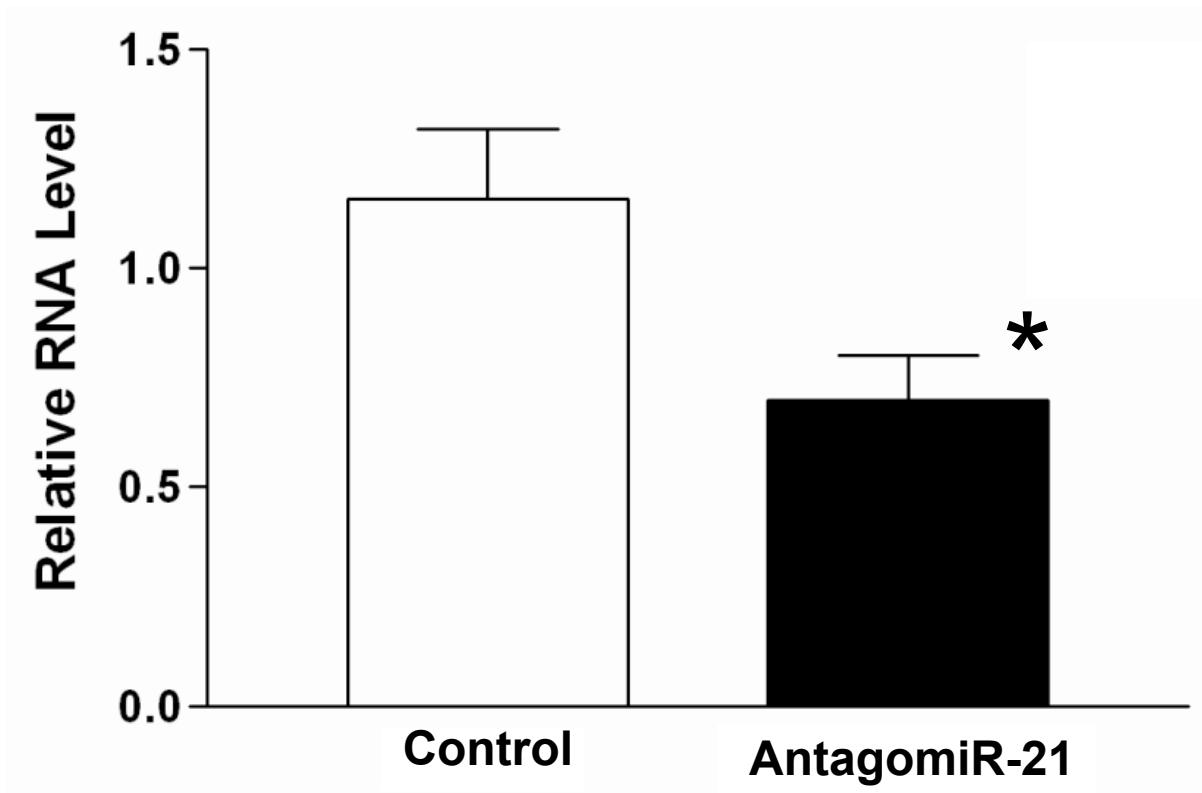


Fig. S3. miR-21 is expressed in mouse cardiac cushion endothelial cells. qPCR from murine cardiac cushion cells demonstrates miR-21 expression, which is reduced upon transfection of a miR-21 antagomir ($P < 0.05$).

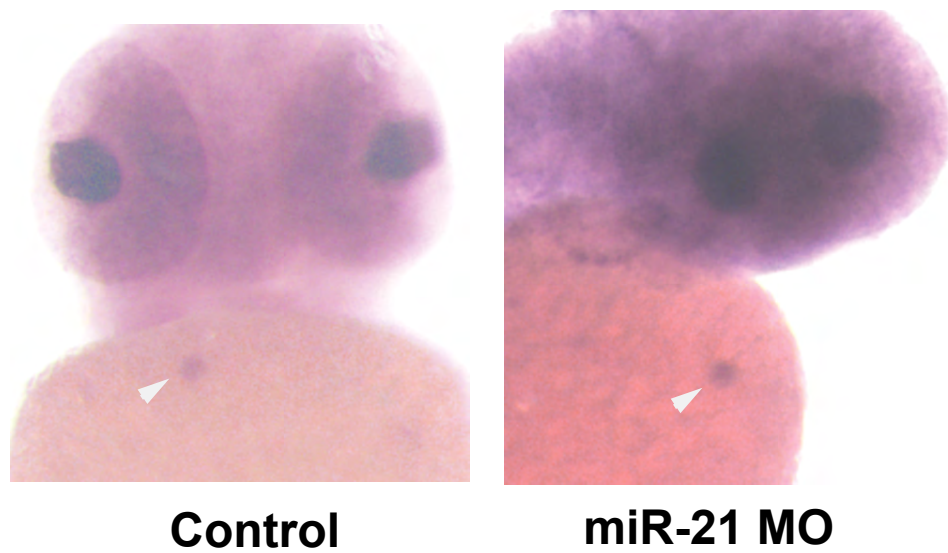
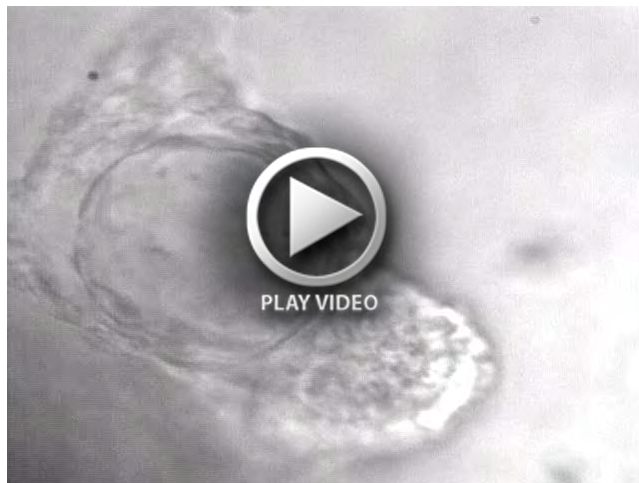


Fig. S4. *In situ* expression pattern of *pcd4b*. Shown are the expression patterns of *pcd4b* under control and miR-21 knockdown conditions.



Movie 1. Control zebrafish embryo heart at 5 days post-fertilization. Atrium is on the left, ventricle on the right.



Movie 2. mirR-21 morphant heart at 5 days post-fertilization. Atrium is on the left, ventricle on the right.



Movie 3. PDCD4-TP^{mir-21} morphant embryo at 48 hours post-fertilization. Atrium is on the right, ventricle on the left.